Journal of Hydrology 606 (2022) 127401

Contents lists available at ScienceDirect

Journal of Hydrology

journal homepage: www.elsevier.com/locate/jhydrol

Research papers

Porewater exchange drives nutrient cycling and export in a mangrove-salt marsh ecotone

Fenfang Wang [a,b], Kai Xiao [c,*], Isaac R. Santos [d,e], Zeyang Lu [a], Joseph Tamborski [f], Yao Wang [a], Ruifeng Yan [a], Nengwang Chen [a,b,*]

[a] Key Laboratory of the Coastal and Wetland Ecosystems, College of the Environment and Ecology, Xiamen University, Xiamen 361102, China
[b] State Key Laboratory of Marine Environment Science, Xiamen University, Xiamen 361102, China
[c] State Environmental Protection Key Laboratory of Integrated Surface Water-Groundwater Pollution Control, School of Environmental Science and Engineering, South University of Science and Technology of China, Shenzhen 518055, China
[d] Department of Marine Sciences, University of Gothenburg, Gothenburg 40530, Sweden
[e] National Marine Science Centre, Southern Cross University, Coffs Harbour, New South Wales 2450, Australia
[f] Department of Ocean & Earth Sciences, Old Dominion University, Norfolk, VA 23529, USA

ARTICLE INFO

This manuscript was handled by Jiri Simunek, Editor-in-Chief, with the assistance of Chunhui Lu, Associate Editor

Keywords:
Blue carbon system
Submarine groundwater discharge
Nitrogen cycle
Denitrification
Zhangjiang Estuary

ABSTRACT

Coastal wetlands regulate nutrient fluxes from the continents to the oceans. Salt marshes are rapidly encroaching into mudflat area in mangrove wetlands, shaping a mangrove-salt marsh ecotone, with unknown implications to coastal biogeochemical cycles. Here, we hypothesized that nitrogen and phosphorus cycling varied in mangrove and salt marsh, having significant implication on coastal waters. We investigated a tidal creek with a marked mangrove-salt marsh gradient in China using high-frequency time-series sampling of dissolved nutrients and observations of porewater exchange rate across the sediment–water interface over a spring-neap tidal cycle. The nitrogen transformation rates and microbiological activities were also investigated to explain the variability in nitrogen concentrations. The mangrove had net groundwater outflow rates of 3.6–4.3 mm d^{-1} while the salt marsh had net infiltration of surface water with rates of 0.5–2.9 mm d^{-1}. Salt marsh had less capacity for ammonium (NH_4-N) production (mineralization and dissimilatory nitrate reduction to ammonium DNRA) than mangrove. Denitrification dominated nitrogen removal reaching 97% and 83% in mangrove and salt marsh, respectively. Microbe distributions were consistent with nitrogen transformations with larger nirS and nrfA abundances for denitrification and DNRA in the mangrove than salt marsh. The mangrove had a net export of NH_4-N but a net import of NO_x-N (sum of nitrate and nitrite) and dissolved inorganic phosphorus (DIP) during the monitoring period. In contrast, the salt marsh had lower efflux of nutrient than influx leading to a net nutrient import during the monitoring period. Porewater released from the mangrove had a large DIN:DIP mole ratio (706 ± 236) due to high NH_4-N concentrations, while NH_4-N in the salt marsh were lower than in the mangrove. Overall, this study revealed that mangrove-salt marsh ecotone will push the native mangrove wetlands from being a source towards a sink of NH_4-N to coastal waters by decreasing porewater exchange, modifying the nutrients stoichiometry, and ultimately alleviating the potential of N-associated eutrophication in nearby coastal waters.

1. Introduction

Mangroves have high productivity and dominate tropical and subtropical shorelines. They were considered as one of the important blue carbon systems which have a high capacity of carbon sequestration and play a key role on regulating nutrient conditions in nearby marine systems (Rogers et al., 2019; Wang et al., 2019). In China, the salt marsh plant *Spartina alterniflora* was introduced in the late 1970s for reducing costal erosion and has spread southward by about 19° of latitude in the last two decades. The alien salt marsh can co-exist with native mangroves due to its strong reproduction and competitive capacity, shaping a typical ecological coexistence phenomenon (i.e., the mangrove-salt

* Corresponding authors at: Key Laboratory of the Coastal and Wetland Ecosystems, College of the Environment and Ecology, Xiamen University, Xiamen 361102, China (N. Chen).
E-mail addresses: xiaok@sustech.edu.cn (K. Xiao), nwchen@xmu.edu.cn (N. Chen).

https://doi.org/10.1016/j.jhydrol.2021.127401
Received 2 July 2021; Received in revised form 12 December 2021; Accepted 24 December 2021
Available online 30 December 2021

marsh ecotone) (An et al., 2007; Zhang et al., 2012). The potential implications of mangrove-salt ecotone to coastal waters are not fully understood, but may alter nutrient cycling and pollution attenuation capacity (Feller et al., 2017; Kelleway et al., 2017).

Submarine groundwater discharge (SGD) and porewater exchange (PEX) play significant roles in material transport and nutrient cycling in mangroves and salt marsh ecosystems (Santos et al., 2019; Tamborski et al., 2021; Xiao et al., 2018). When the spatial scale is equivalent to a meter or larger than meters, it is referred to as SGD (Moore, 2010). When the scale is smaller than meters and the time scale is shorter than days or hours, porewater flows are often referred to as PEX (Taniguchi et al., 2019). Both SGD and PEX transport nutrients from wetland to coastal waters, often enhancing productivity and sometimes driving harmful algal blooms and eutrophication (Dittmar & Lara, 2001; Santos et al., 2014). Groundwater discharge also modifies DIN:DIP ratios with implications to the composition of biological communities in nearshore waters (Tait et al., 2017; Xiao et al., 2019).

Tides control PEX and thus alter biogeochemical parameters such as salinity, pH, and redox potential (Robinson et al., 2007; Taniguchi, 2002). These parameters can affect microbial communities which modify essential biogeochemical processes of nitrogen cycling such as nitrification of NH_4-N to NO_3-N, denitrification of NO_3-N to N_2O or N_2, dissimilatory nitrate reduction to ammonium (DNRA) of NO_3-N to NH_4-N, anaerobic ammonium oxidation (anammox) of NH_4-N and NO_2-N to N_2 and the coupled nitrification–denitrification processes in sediments (Slomp & Van Cappellen, 2004; Xiao et al., 2018).

Microbial species, carbon and nutrient cycling, and other physicochemical characteristics differed in salt marsh and mangrove due to the different traits of vegetation and the hydrological conditions (Cui et al., 2021; Steinlein, 2013). Studies showed that fine roots of herbaceous salt marsh plants are likely to increase the capacity to retain water (Liu et al., 2020), affecting the hydraulic characteristics. The differences in carbon quality between salt marsh (C4 plant) and mangrove (C3 plant) lead to variations in carbon and nitrogen storage (McKee & Vervaeke, 2018; Yang et al., 2013). Functional gene abundance in sediments responsible for nitrogen transformations also varied, leading to the difference in the nitrogen cycling between salt marsh and mangrove (Gao et al., 2019; Zhang et al., 2011). However, the interplay among PEX, tidal types, and biochemical processes on nutrient source-sink patterns remains poorly understood in the context of changing mangrove-salt marsh ecotone.

Here, we hypothesized that salt marsh growth in mangrove-dominated wetlands will modify PEX and nutrient biogeochemistry. We investigated PEX, nitrogen transformations and associated microbiological activities in a subtropical mangrove wetland being invaded by salt marshes in Southeast China. We carried out time-series observations of nutrient concentrations in surface water and shallow groundwater (i.e., porewater) during a spring-neap tide cycle. The specific objectives of this study were: (1) to estimate PEX-derived nutrient fluxes across the Sediment-Water Interface (hereafter "SWI") in the mangrove and salt marsh; (2) to explore the hydro-biogeochemical controls of the nutrient export or import patterns across SWI and (3) to discuss the potential ecological and environmental implications of mangrove-salt marsh ecotone to coastal waters.

2. Materials and methods

2.1. Description of study site

The study site was in Zhangjiang Estuary National Mangrove Reserve (ZJENMR) (117°24′-117°30′E, 23°53′–23°56′N) in Southeast China

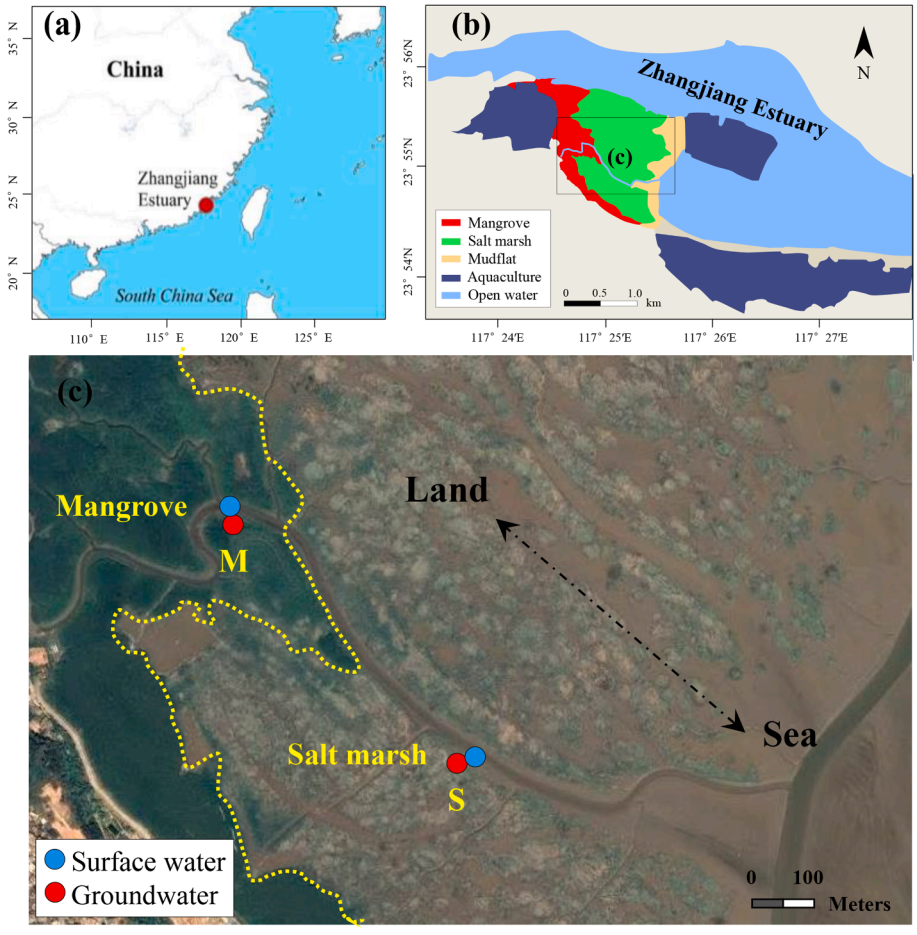

Fig. 1. Map of study area: (a) the location of study area to the South China Sea; (b) mangrove-salt marsh ecotone location relative to Zhangjiang estuary; (c) the spatial distribution of study sites. The surface elevation at M was about 15 cm higher than at S. The yellow dotted line indicates the approximate boundary between native mangroves (left area) and salt marshes (right area). (For interpretation of the references to color in this figure legend, the reader is referred to the web version of this article.)

(Fig. 1). The mangrove wetland covers an area of ~2.6 km^2 and experiences a semidiurnal tide with a tidal range of 0.43–4.67 m (2.32 m on average) (Zhu et al., 2019). The region is subject to a subtropical monsoon climate, with an annual mean air temperature of 22.8 °C, and average precipitation of 1680 mm. The dominant mangrove species are *Kandelia candel*, *Avicennia marina* and *Aegiceras corniculatum*. *Spartina alterniflora* is invading into mudflat areas at the edge of mangroves. The invasive area has increased to 1.4 km^2 over the last 30 years (Dong et al., 2020).

2.2. Monitoring and sampling campaigns

Field observations were conducted along a winding tidal creek forming a natural ecological continuum of mangrove-salt marsh (Fig. 1). The approach for quantifying PEX rate relied on data from two "paired-wells" installed along the creek edges of the mangrove and salt marsh (Fig. S1). The paired-wells (70 cm depth) were equipped with inner (Φ 30 mm) and outer (Φ 100 mm) plexiglass pipes (Fig. S1). Two CTD-Diver loggers (vanEssen, Netherlands) were installed in the inner pipes at the depths of 5 cm (upper sensor) and 65 cm (lower sensor) to record water temperature, conductivity and pressure, and one at the bottom of the creek to monitor tidal fluctuations. To minimize the impact of sediment disturbance, monitoring began two days after installation at a frequency of 30 min. The monitoring occurred on two occasions, including one day during neap tides on 10th October 2020, and a day during spring tides on 20th October 2020.

Surface water was collected hourly during the monitoring periods using a Niskin hydrophore. Groundwater at 25–50 cm depth was collected hourly from adjacent sampling wells using a peristaltic pump (Fig. S2). All samples were filtered with a GF/F membrane (0.7 μm) and stored at 4 °C until analysis for nutrients. Temperature, dissolved oxygen (DO), and salinity were measured *in-situ* using a portable meter (Multi 3430, Germany).

Samples for analyzing dissolved N_2 gases were first introduced into 12 mL LABCO exetainer vials through a silicone tube. Then, $HgCl_2$ with a concentration of 0.1% was added to prevent microbial activity (Chen et al., 2014). All the bottles were stored in fresh water to maintain *in-situ* temperature. Sediment cores were collected using a plexiglass pipe (Φ120 mm × 500 mm) near the groundwater sampling sites on 21st October 2020 to depths of 20–30 cm. Subsamples for nitrogen transformation incubation and physicochemical analysis were stored at 4 °C. Secondary subsamples for the analysis of nitrogen functional gene abundance were stored at −20 °C (Wang et al., 2019).

2.3. Laboratory analysis and PEX rate

Nitrate (NO_3-N), nitrite (NO_2-N), ammonium (NH_4-N), total dissolved nitrogen (TDN), dissolved reactive phosphorus (DRP) and total dissolved phosphorus (TDP) were analyzed by segmented flow colorimetry (San++ analyzer, Germany). TDN and TDP concentrations were determined as NO_3-N and DRP following oxidization with 4% alkaline potassium persulfate. Dissolved inorganic nitrogen (DIN) was the sum of NO_3-N, NO_2-N and NH_4-N. Dissolved organic nitrogen (DON) and dissolved organic phosphorus (DOP) were taken as the difference between TDN and DIN and between TDP and DRP respectively. The precision was determined by repeated determination of 10% of the samples and the relative error was 3%–5%. Dissolved N_2 concentrations were measured using the N_2:Ar method in a membrane inlet mass spectrometer (Chen et al., 2014). Details about the calculation of excess production of N_2 (ΔN_2) are shown in supporting information (Text S1).

Potential rates in sediments of denitrification, anammox and DNRA were determined by the nitrogen isotope-pairing technique (Hou et al., 2016; Yin et al., 2015). The rates of mineralization and nitrification were quantified by nitrogen isotope dilution (Lin et al., 2016; Lin et al., 2021) as explained in detail in Text S2. Sediments for total organic carbon (TOC) were freeze-dried and then ground before analysis. The subsample of ground sediments was acidified with 1 M HCl and TOC was determined by an element analyzer-IRMS (PE2400 SERIESIICHNS/O). Another subsample of ground sediments was measured for Eh after the pretreatment with mixing water and sediments in a ratio of 1:5 using a WTW multiparameter (Multi 3430, Germany).

FastDNA™ Spin Kit for Soil (Millipore, USA) was used to extract DNA. The extracted DNA was suspended in 50 μL TE solution and stored at about −80 °C until analysis. The concentrations of DNA were quantified by Nano Drop spectrophotometer (DN-1000; Isogen Life Science, the Netherlands). Bio-Rad CFX96 qPCR (USA) was used for qPCR amplification for functional gene abundance. Primer pairs used to quantify gene abundance are shown in Table S1.

The hydraulic gradient between the upper and lower wells was estimated based on the generalized form of Darcy's law and the vertical hydraulic conductivity was obtained from the in-situ falling head method to calculate vertical PEX rates (Qu et al., 2017) with details in supporting information (Text S3). The steepness of sampling sites were measured by the method introduced in Text S4.

3. Results

3.1. Physicochemical parameters and nutrients

During neap tides, salinity in salt marsh was 8% higher than in mangrove without obvious difference between surface water and groundwater (Table S1). During spring tides, the salinity in salt marsh groundwater was similar to surface water, 10% greater than in mangrove groundwater while comparable to the mangrove surface water. The DO in mangrove groundwater was significantly lower than that in surface water ($p < 0.05$), but no differences were observed within tidal cycles (i.e., between neap and spring tides) (Fig. 2). The salt marsh had similar DO concentrations to the mangrove in surface water and no significant difference occurred with tidal cycles ($p > 0.05$).

Nutrient concentrations varied with tidal cycles, water types, and ecosystems (Fig. 2 and Table 1). In the mangrove, the dominant form of DIN was NO_3-N (59%–60%) in surface water and NH_4-N (70%–99%) in groundwater. In the salt marsh, NO_3-N was the main form (>50%) in both surface water and groundwater (Fig. S3). NH_4-N at low tides was 85%–94% higher than at high tides in mangrove surface water (Table S3). NH_4-N in mangrove groundwater was 5.7 times higher than in surface water. NH_4-N concentration in salt marsh surface water was close to that in mangrove surface water. NH_4-N concentration in marsh groundwater was comparable to (spring tides) or slightly lower (neap tides) than that in surface water, and significantly lower than mangrove groundwater ($p < 0.05$). NO_x-N concentration (the sum of NO_3-N and NO_2-N) during neap tides (51.0 ± 12.0 μmol L^{-1}) was similar to spring tides (49.8 ± 6.5 μmol L^{-1}) in mangrove surface water. NO_x-N concentration at low tides was 71%–97% lower than that at high tides. NO_x-N concentration in mangrove groundwater was 55% and 97% lower than in surface water during neap and spring tides, respectively. The salt marsh and mangrove had similar NO_x-N concentration in surface water (50–60 μmol L^{-1}). DON in surface water and groundwater of the mangrove and salt marsh were similar during spring tides (17–27 μmol L^{-1}), but during neap tides, DON in surface water (3.7–11.7 μmol L^{-1}) was much lower than that in groundwater (206.3–297.1 μmol L^{-1}).

In mangrove surface water, DRP during neap tides (2.6 ± 0.4 μmol L^{-1}) was higher than that during spring tides (2.1 ± 0.4 μmol L^{-1}). DRP in mangrove groundwater had no obvious difference between spring and neap tides, but was one order of magnitude lower than surface water. In the salt marsh, DRP in surface water and groundwater were lower than that of the mangrove during neap tides (Table 1). DRP concentration during spring tides was much higher than that during neap tides without obvious difference between surface and groundwater.

DIN:DIP mole ratios in groundwater were much larger than that in surface water both in the mangrove and salt marsh (Fig. S4). DIN:DIP mole ratios in mangrove groundwater were 30 and 15 times larger than

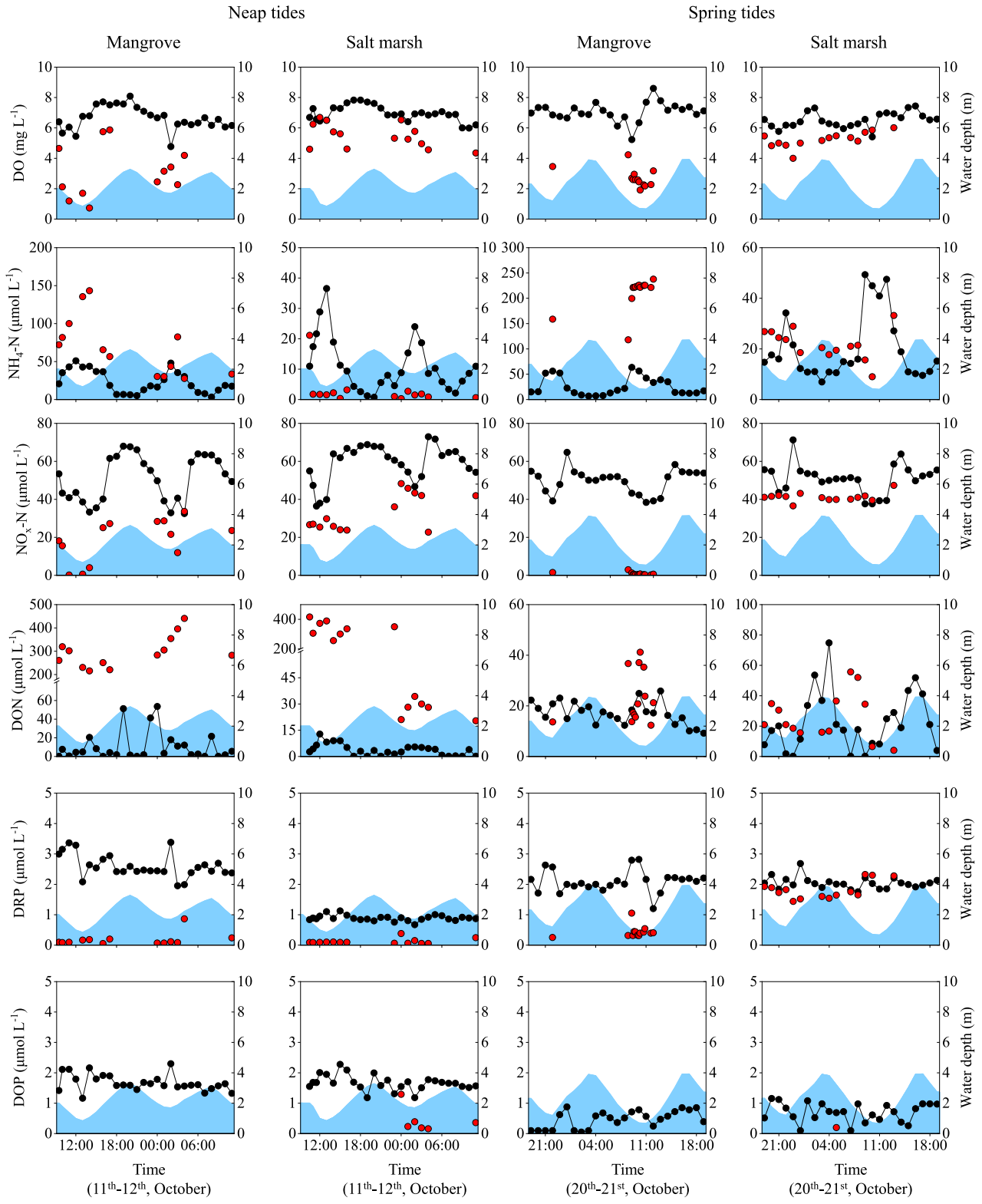

Fig. 2. Tidal variations of water depth, DO, and concentrations of nitrogen and phosphorus in surface water (black circles) and groundwater (red circles) in the mangrove and salt marsh during neap (11^{th}-12^{th}, October 2020) and spring (20^{th}-21^{st}, October 2020) tides. Most of DOP in groundwater were under the detectable level. (For interpretation of the references to color in this figure legend, the reader is referred to the web version of this article.)

that in surface water during neap and spring tides, respectively. In salt marsh, DIN:DIP mole ratios in groundwater were 6 and 3 times larger than in surface water during neap and spring tides, respectively, but both were much lower than that in mangrove groundwater.

3.2. Hydrodynamics and PEX

Water depths varied from 0.85 m to 3.28 m during neap tides and 0.68 m to 3.93 m during spring tides. The inundation time of the

Table 1
Mean (±SD) salinity, DO and concentrations of NH_4-N, NO_x-N, DON, DRP, and DOP in surface water (SW) and groundwater (GW) in the mangrove (M) and salt marsh (S) during neap and spring tides. The values marked by "*" mean significant difference during the same water types in different tidal types at $p < 0.5$.

Date	Tidal types	Water types	Salinity	DO	NH_4-N	NO_x-N	DON	DRP	DOP
				mg L^{-1}	μmol L^{-1}				
2020–10-11	Neap	SW-M	(16.7 ± 1.6)*	(6.7 ± 0.8)	(23.2 ± 14.8)	(51.0 ± 12.0)	(11.7 ± 15.8)	(2.61 ± 0.37)*	(1.67 ± 0.27)*
		GW-M	(16.2 ± 0.8)*	(3.1 ± 1.7)	(69.4 ± 38.7)*	(22.9 ± 13.4)*	(297.1 ± 67.7)*	(0.18 ± 0.21)	(0.00 ± 0.12)
		SW-S	(17.5 ± 2.0)*	(7.0 ± 0.5)	(11.3 ± 8.9)	(58.9 ± 10.1)	(3.7 ± 3.3)*	(0.89 ± 0.09)*	(1.67 ± 0.25)*
		GW-S	(17.8 ± 0.8)*	(5.5 ± 0.8)	(2.9 ± 5.3)*	(40.6 ± 13.1)	(206.3 ± 65.6)*	(0.12 ± 0.09)*	(0.44 ± 0.43)*
2020–10-20	Spring	SW-M	(21.2 ± 1.6)	(7.1 ± 0.6)	(26.0 ± 18.2)	(49.8 ± 6.5)	(17.1 ± 4.5)	(2.09 ± 0.36)	(0.47 ± 0.29)
		GW-M	(19.0 ± 0.5)	(2.5 ± 0.9)	(209.5 ± 33.7)	(1.3 ± 1.0)	(23.5 ± 10.4)	(0.43 ± 0.20)	(0.00 ± 0.30)
		SW-S	(21.2 ± 1.8)	(6.5 ± 0.5)	(19.6 ± 12.7)	(51.3 ± 7.7)	(22.4 ± 18.8)	(2.04 ± 0.19)	(0.65 ± 0.39)
		GW-S	(21.2 ± 1.4)	(5.2 ± 0.5)	(22.5 ± 6.3)	(48.0 ± 2.5)	(27.4 ± 16.0)	(1.66 ± 0.50)	(0.00 ± 1.35)

mangrove (14 h) was shorter than that in the salt marsh (20 h) without a significant difference between neap and spring tides. The direction and magnitude of PEX across the SWI were variable (Fig. S5). The vertical hydraulic conductivity (K_v) in the salt marsh was slightly larger than that in the mangrove (Table S2). The average outflow rates (0.75 and 0.41 mm h^{-1} during neap and spring tides, respectively) in the mangrove were larger than inflow rates (0.20 and 0.20 mm h^{-1}) during both neap and spring tides (Fig. S5), resulting in a net discharge of groundwater during both tides. During spring tides, the exchange between groundwater and surface water approached stagnation in salt marsh. On comparison, the exchange between groundwater and surface water became active during neap tides. For example, the inflow rate (0.26 mm h^{-1}) of surface water was larger than outflow rate (0.15 mm h^{-1}) of groundwater, resulting in a net infiltration of surface water into marsh sediments. This could be explained by the larger slope of creek bank in the mangrove (steepness: 4.6%) than salt marsh (steepness: 3.6%), leading to larger hydraulic gradient between tidal creek and monitoring sites in the mangrove and salt marsh (Fig. 1).

3.3. Nutrient fluxes via PEX

The magnitude and direction of nutrient fluxes driven by PEX varied with nutrient species and tidal types (Fig. 3, Fig. 4 and Table S4). In the mangrove, NH_4-N and DON were exported from groundwater to surface water. The net groundwater efflux of NH_4-N during spring tides was almost twice than that during neap tides. In contrast, the net efflux of DON during neap tides was two orders of magnitude larger than that during spring tides. NO_x-N was imported into groundwater from surface water. Overall, TDN had net efflux during both neap (2.6 mmol m^{-2} d^{-1}) and spring tides (1.1 mmol m^{-2} d^{-1}) (Fig. S5). In the salt marsh, most forms of nitrogen were imported into sediments from surface water except DON during neap tides and NH_4-N during spring tides.

All forms of phosphorus had net influx but varied with ecosystems and tidal types. The net influx of DIP in the mangrove was 28%-36% larger than that in the salt marsh. In contrast, DOP had 31%-51% larger net influx in the salt marsh than that in the mangrove. The net influx of TDP in the mangrove (9.8×10^{-3} mmol m^{-2} d^{-1}) was 11% smaller than that in the salt marsh (1.1×10^{-2} mmol m^{-2} d^{-1}) during neap tides, while 9% larger during spring tides (2.3×10^{-3} and 2.1×10^{-3} mmol m^{-2} d^{-1}) (Fig. S5).

3.4. Nitrogen transformation and functional gene abundance in sediments

The potential rates of nitrogen transformations and associated functional gene abundance in sediments varied with ecosystems (Table S5). In mangrove sediments, mineralization was the dominant process at 14.03 ± 1.12 μmol $kg^{-1}h^{-1}$, followed by denitrification (7.49 ± 0.71 μmol $kg^{-1}h^{-1}$), DNRA (4.85 ± 0.76 μmol $kg^{-1}h^{-1}$), nitrification (4.51 ± 2.43 μmol $kg^{-1}h^{-1}$), and anammox (0.24 ± 0.01 μmol $kg^{-1}h^{-1}$). The rates in salt marsh sediments were all smaller than those in mangrove except anammox at 1.03 ± 0.09 μmol $kg^{-1}h^{-1}$. The potential rate of nitrification was undetectable in salt marsh sediments.

The dominant microbes for nitrification were ammonia-oxidizing archaea (AOA) and nitrite-oxidizing bacteria (NOB) in both mangrove (1.96×10^6 and 3.07×10^6 copies g^{-1} wet soil) and salt marsh sediments (0.7×10^6 and 0.49×10^6 copies g^{-1} wet soil) (Table S5). Ammonia-oxidizing bacteria (AOB) was two orders of magnitude lower than AOA and NOB in both the mangrove (7.90×10^4 copies g^{-1} wet soil) and salt marsh sediments (1.60×10^4 copies g^{-1} wet soil). nirS was the dominant gene for denitrification, and the relative abundance in the mangrove (1.12×10^8 copies g^{-1}) was larger than that in the salt marsh (0.15×10^8 copies g^{-1}). narG (another functional gene for denitrification) was two orders of magnitude lower than nirS, but the larger value also occurred in mangrove sediments (8.18×10^6 copies g^{-1}). The gene abundance of hzsB for anamox and nrfA for DNRA in mangrove sediments was about four times and seven times higher than that of the salt marsh.

The accumulation and removal of nitrogen and associated contributions of transformation processes varied in mangrove (Fig. 5a) and salt marsh sediments (Fig. 5b). Mineralization (84%) was the main contributor to NH_4-N production in the mangrove, while in the salt marsh DNRA (62%) exceeded mineralization (38%). Nitrification was the major process for NH_4-N consumption in mangrove sediments while anammox was greater in salt marsh sediments. Denitrification played a dominant role in NO_3-N removal compared to DNRA. The contribution of denitrification in mangrove sediments was slightly larger than that in salt marsh sediments. Considering the production and removal processes, the net accumulation of NH_4-N in mangrove sediments (14.3 μmol $kg^{-1}h^{-1}$) was larger than that in salt marsh sediments (7.1 μmol $kg^{-1}h^{-1}$). In contrast, the removal of NO_3-N in salt marsh sediments was larger than that in mangrove sediments.

4. Discussion

4.1. Hydro-biogeochemical control on porewater nitrogen

Tides were the main factor driving the vertical PEX. The mangrove had net groundwater efflux, while the salt marsh had net surface water influx during the monitoring period (Fig. 3). The salt marsh had a smaller PEX due to the smaller hydraulic gradient than mangrove. This further indicated that the hydraulic gradient played a critical role in regulating PEX when the similar hydraulic conductivity exited in two coastal habitats. In addition, the surface elevation of the salt marsh was about 15 cm lower than that of the mangrove, resulting in longer water inundation period. Smaller differences in salinity between surface water and groundwater (Table 1) suggest a larger proportion of seawater in the groundwater in the salt marsh than in the mangrove. All in all, the different geological setting in two ecosystems led to different hydrology including water residence time and flow rate that control biogeochemical properties in sediments.

Nitrogen cycling on intertidal sediments is highly dynamic with large temporal and spatial variability controlled by sediment permeability, transport mechanisms, tidal cycles, vegetation types and microbial activities (Schutte et al., 2019). Mineralization and DNRA are two major

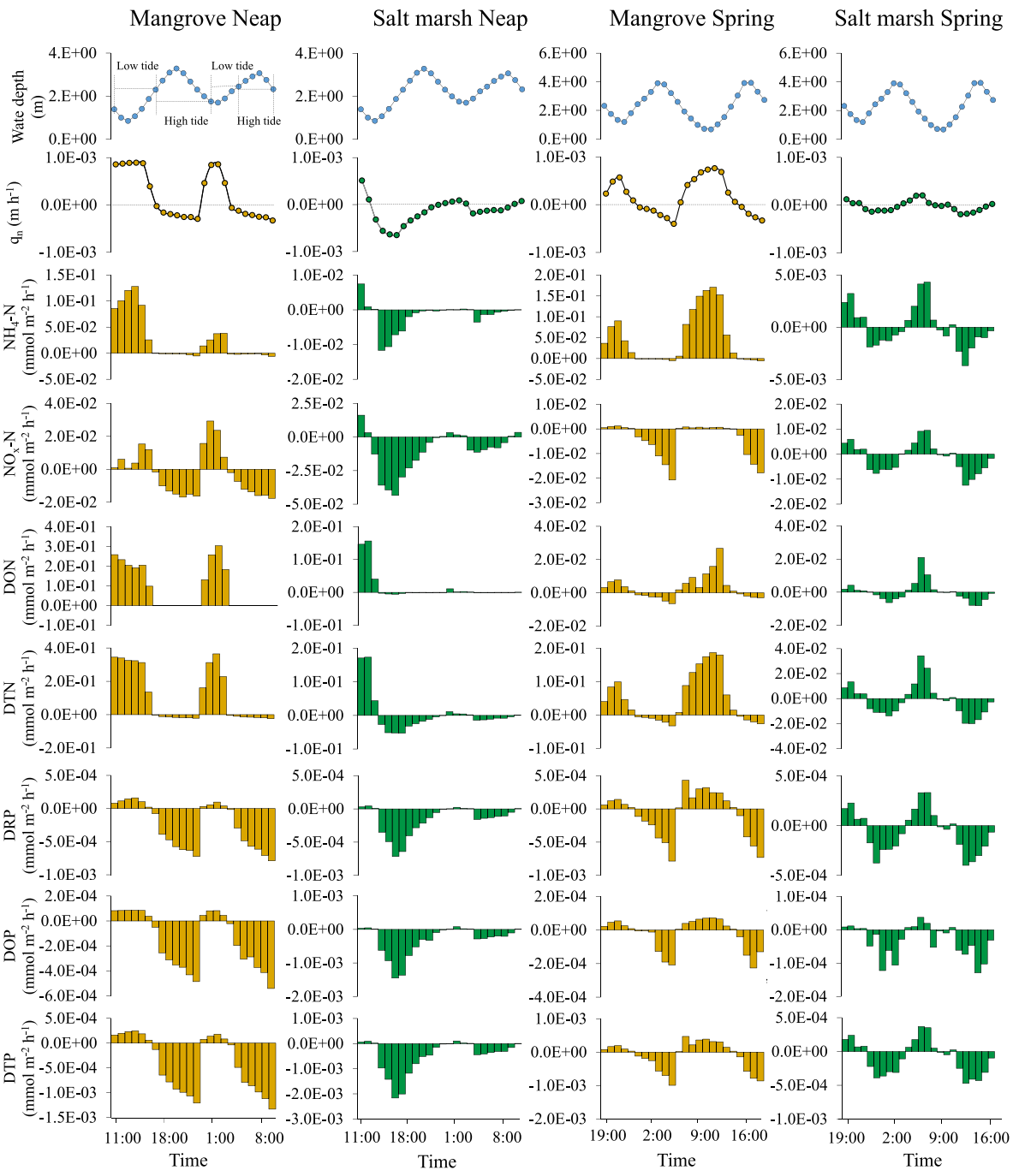

Fig. 3. Time series of water depth in the tidal creek and hourly nutrient fluxes in the mangrove (yellow bars) and salt marsh (green bars) during neap tides (11^{th}-12^{th}, October 2020) and spring tides (20^{th}-21^{st}, October 2020). The positive and negative values indicate the groundwater efflux and surface water influx, respectively. (For interpretation of the references to color in this figure legend, the reader is referred to the web version of this article.)

processes controlling NH_4-N production, while nitrification and anammox controlled NH_4-N loss in sediments (Fig. 5). TOC was the substrate for mineralization, and strong mineralization often results in high NH_4-N in porewater (Lee et al., 2008; Wang et al., 2019). Higher TOC contents explained larger rates of mineralization in mangrove (14.03 μmol $kg^{-1}h^{-1}$) than salt marsh (2.71 μmol $kg^{-1}h^{-1}$) (Table S5). Functional gene abundances and potential nitrogen transformation rates had a significant positive correlation ($n = 7$; $R^2 = 0.58$, $p < 0.05$) (Fig. S6). Higher gene abundance of nrfA (DNRA gene) was also observed in mangrove sediments than in the salt marsh (Table S5), explaining larger DNRA in the mangrove. All the above contents explained NH_4-N concentrations in groundwater were larger in the mangrove than in the salt marsh.

While anaerobic conditions are expected in wetland sediments, the mixing of groundwater (low DO) and surface water (high DO) enable nitrification in sediments (Xiao et al., 2018). Shorter residence time of groundwater and the longer unsubmerged time caused by higher elevation in the mangrove increased oxygen penetration, leading to higher Eh and nitrifying bacteria (AOA, AOB and NOB) than in salt marsh sediments (Table S5). The previous study in the same study area showed water contents and salinity in salt marsh sediments were larger than in mangrove sediments (Gao et al., 2019). Larger water content blocks the penetration of oxygen, resulting a prolonged anaerobic state

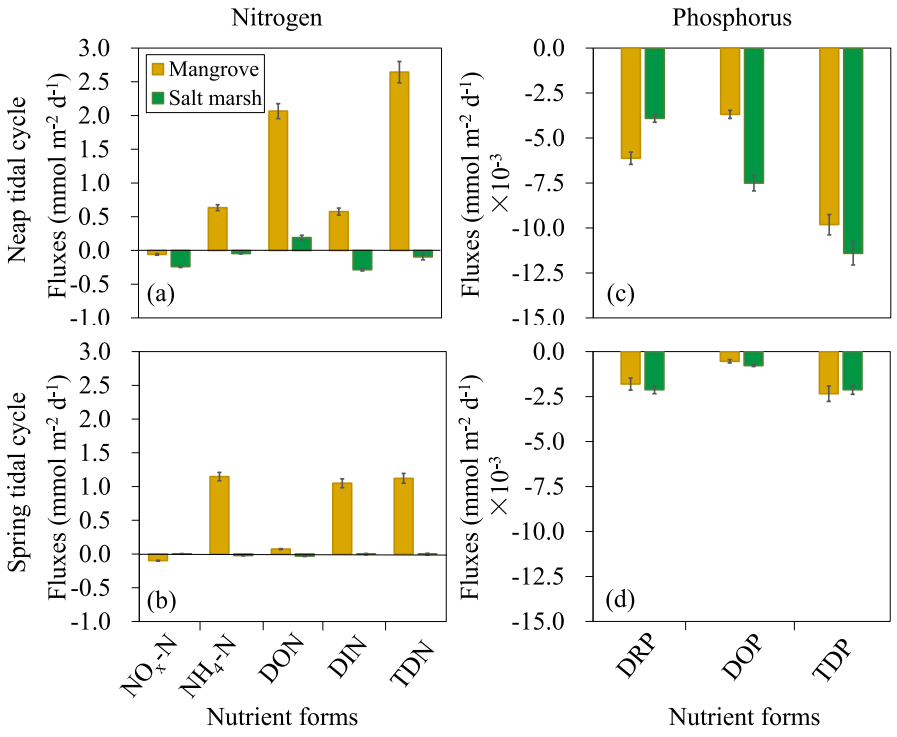

Fig. 4. The net fluxes of nutrients across the SWI in the mangrove and salt marsh during neap and spring tides. Positive and negative values indicate the groundwater efflux (i.e., export) and surface water influx (i.e., import).

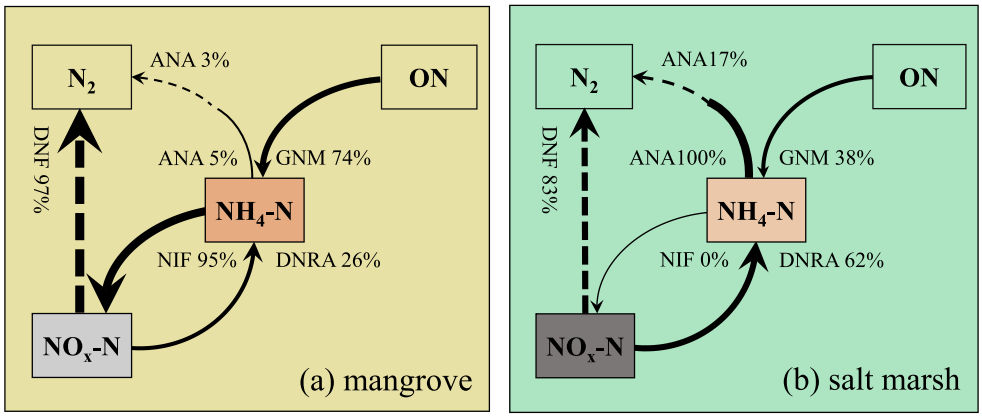

Fig. 5. The relative contributions of mineralization (GNM), dissimilatory nitrate reduction to ammonium (DNRA), nitrification (NIF), and anammox (ANA) to NH_4^+-N addition or removal (solid lines), and the contributions of denitrification (DNF) and ANA to N_2 production (dotted lines) in the (a) mangrove and (b) salt marsh. The squares with darker color present more removal (grey color) of NO_3-N or more accumulation (orange color) of NH_4-N. ON means organic nitrogen. (For interpretation of the references to color in this figure legend, the reader is referred to the web version of this article.)

of sediments and low nitrification potential. Study showed that nitrification process generally decreased with increasing salinity (Meng et al., 2020). These above factors explained higher nitrification potential in the mangrove than in the salt marsh.

Both gene abundance and activities of anammox microbes can have a positive correlation with the sediment organic carbon (Lisa et al., 2014). Mangrove has C3 photosynthesis and can retain its aboveground biomass in the whole year, while salt marsh conducting C4 photosynthesis has to regrow after the senescence in winter (McKee & Vervaeke, 2018). The difference in photosynthesis lead to higher TOC accumulation in mangrove sediments than in salt marsh sediments (Table S5). Richer TOC in mangrove explained higher gene abundance of hzsB than in salt marsh. Salinity, water content, redox potential and the concentration of NO_2-N in sediments also affect anammox bacteria activities (Dale et al., 2009; Shen et al., 2017; Zhang et al., 2020). NO_2-N is an important oxidized substrate for anammox (Risgaard-Petersen et al., 2003). NH_4-N is usually plentiful in sediments, while NO_2-N likely controls the gene abundance for anammox (Luvizott et al., 2019). Much lower NO_2-N in mangrove groundwater than that in marsh groundwater may lead to lower anammox potential in mangrove sediments. There was a greater net accumulation of NH_4-N in mangrove sediments than in the salt marsh (Fig. 5a-b). Taken together, these lines of evidence help to explain higher NH_4-N in groundwater than surface water and lower concentrations in marsh groundwater than in mangrove groundwater.

NO_x-N in groundwater was lower compared to that in surface water (Fig. 2) because denitrification, anammox and DNRA remove NO_x-N in anaerobic conditions. Potential denitrification accounted for 97% and 83% of nitrogen removal in mangrove and marsh sediments, respectively. In line with our previous observations in another eutrophic Chinese estuary, invasive salt marshes can have higher denitrification rates than the unvegetated zone, but lower rates than the native mangrove zone (Wang et al., 2014).

Denitrification rates were correlated positively with functional genes as observed in other studies focused on estuarine wetlands in China and

the U.K. (Gao et al., 2017; Smith et al., 2015). Here, the gene abundance of narG and nirS in mangrove sediments were all higher than that in the salt marsh (Table S5). NO_x-N can be reduced to N_2 via denitrification. We indeed observed higher dissolved nitrogen gas (ΔN_2) in mangrove groundwater than marsh groundwater over time-series observation (Fig. S7). Compared with denitrification, DNRA played a less role in NO_3-N removal in both mangrove and salt marsh (Fig. 5). The lower DNRA rate in salt marsh sediments is consistent with earlier observation that the invasion of *Spartina alterniflora* can minimize DNRA (Gao et al., 2019).

Water exchange across the SWI has a negative correlation with groundwater residence time (Qu et al., 2017). Water residence time affects the duration and frequency of anaerobic/aerobic conditions, which then alters nitrogen cycling including aerobic nitrification and anaerobic denitrification (Pezeshki, 2001; Sharp et al., 2021). Overall, longer groundwater residence time usually increases nitrogen removal (Sharp et al., 2021). The lower exchange rates in the mangrove during spring tides than neap tides suggested longer groundwater residence time, causing oxygen consumption and NO_x-N removal via denitrification (Gonneea & Charette, 2014), explaining lower NO_x-N in groundwater during spring tides.

4.2. Contrasting nutrient fluxes via PEX between mangrove and salt marsh

Our estimated PEX rates and nutrient fluxes fell well within the wide range observed in other intertidal wetlands (Table 2). However, our DIN fluxes were lower than most other investigations due to the lower nitrogen concentrations or PEX rates with the exception in Jiaozhou Bay, China. For example, average NH_4-N and NO_x-N in groundwater in Dan'ao Estuary, China was 200 and 350 μmol L^{-1}, about 3 and 12 times greater than in our study. Combined with the two orders of magnitude larger PEX, much larger nutrient fluxes were estimated for Dan'ao Estuary (Li et al., 2018). Though the nitrogen concentrations were 10–20 times higher in Jiaozhou Bay, the PEX was two orders of magnitude lower than this study, driving lower nutrient fluxes (Qu et al., 2017).

The mangrove had a net export of NH_4-N and a net import of NO_x-N (Fig. 4). This finding supports recent observations of NH_4-N exports and NO_x-N imports into mangrove creeks (Wadnerkar et al., 2019; Wang et al., 2021). During neap tides, the average water level is relatively low, resulting in large hydraulic gradient between groundwater and surface water in the tidal creek, leading to a greater efflux and explaining the stronger source of nitrogen during neap tides than spring tides. Net influx of NH_4-N, NO_x-N, DIN and TDN in the salt marsh signified the salt marsh served as a sink of nitrogen during our observations. A smaller hydraulic gradient, proximity to the sea and possibly longer water residence time than in mangrove, drove nitrogen infiltration in the salt marsh. A correlation analysis (Fig. S8) implied that the net efflux or influx of DIN and TDN were controlled by PEX. However, the high denitrification rates reducing NO_x-N concentrations in groundwater played a more significant role in NO_x-N fluxes than the magnitude of PEX.

Both the mangrove and salt marsh had a net import of dissolved phosphorus (Fig. 4). The concentrations of DIP and DOP in surface water were all much greater than those in groundwater, implying P retention in sediments. Phosphorus in sediments can be controlled by the immobilization of Ca or Fe species, and adsorption or desorption of suspended particles (Ranjan et al., 2011; Smolders et al., 2017). A previous study in the same study area showed that a large amount available phosphorus were utilized or transferred from the sediments to the plants, leading to a decrease in phosphorus contents in sediments (Feng et al., 2017). Lower DIP in groundwater than surface water in our study may be the result of strong uptake by plant roots and microorganisms. Physical absorption by sediment particles and chemical immobilization could also reduce DIP in groundwater (Holmboe et al., 2001). We hypothesized that the extensive removal activities in salt marsh sediments subsequently led the salt marsh to become a DIP sink when surface water contains high nutrient concentration that infiltrates into sediments. The larger difference in concentrations between surface water and groundwater indicated a larger net import of DIP during neap tides than spring tides.

4.3. Uncertainty analysis

Organic matter degradation and nutrient cycling varied seasonally in intertidal groundwater due to the seasonal differences in rainfall, temperature and plant periodicity growth (Steinmuller et al., 2020; Sullivan et al., 2021; Wang et al., 2019). Our previous study along the tidal creek in the same area showed that the nutrient concentrations at high tides were similar among seasons, but the concentrations at low tides showed seasonal variations with the largest variation of 80%, which were likely affected by the groundwater discharge (Wang et al., 2019). We assumed that there were no significant seasonal variations of nutrient concentrations in surface water. We set the seasonal variations of groundwater concentrations to ± 25%, ±50% and ± 80% to analyze the nutrient fluxes across the SWI (Fig. S9). The results showed that in mangrove NO_3-N always had net influxes, while NH_4-N, DIN and TDN always had net efflux during both neap and spring tides, which were consistent with the results observed in this study. In salt marsh, the pattern of nitrogen fluxes were almost the same as that in this study with an exception of TDN (Fig. S9 g). Patterns of phosphorus fluxes in mangrove and salt marsh were not affected by the alteration in concentrations during neap tides (Fig. S10 a-h). During spring tides, the influx of phosphorus in salt marsh shifted from less to larger than in mangrove when the concentrations in mangrove and salt marsh groundwater both increased by over 25% (Fig. S10 l-n). Overall, the seasonal variations in nutrient concentrations caused by discrepancy in plant uptake and microbial activities

Table 2
Comparisons of PEX, and fluxes of DIN and DIP with previous wetland studies.

Study area	Wetland types	PEX (cm d^{-1})	Fluxes (mmol m^{-2} d^{-1})		References
			DIN	DIP	
Clarence River estuary, Australia	Mangrove	1.3–3.4	0.32	n. a.	Wadnerkar et al. (2021)
Coffs Creek, Australia	Mangrove	n. a.	0.05	0.01	Reithmaier et al. (2021)
Kooragang Island, Australia	Mangrove	14.0	21.00	n. a.	Sadat-Noori and Glamore (2019)
Tauranga Harbor, New Zealand	Mangrove	8.0–34.0	n. a.	n. a.	Santos et al. (2014)
Kangaroo Island, Australia	Mangrove	7.4–16.2	1.23–2.29	0.30–0.38	Gleeson et al. (2013)
~12.4 S-~38.3 S, Australia	Mangrove	1.5–30.9	9.00	0.95	Tait et al. (2017)
Daya Bay, China	Mangrove	0.06–3.3	n. a.	n. a.	Xiao et al. (2018)
Dan'ao estuary, China	Mangrove	31.4	160.30	14.60	Li et al. (2018)
Zhangjiang Estuary, China	Mangrove	0.4	0.08	0.12	This study
Massachusetts, US	Salt marsh	3.0	4.66–19.45	0.36–14.76	Charette (2007)
North inlet, US	Salt marsh	3.2	2.42	0.91	Krest et al. (2000)
Jiaozhou Bay, China	Salt marsh	3.6×10^{-3}	0.03	6.00×10^{-5}	Qu et al. (2017)
Zhangjiang Estuary, China	Salt marsh	0.2	0.04	0.85×10^{-2}	This study

Note: "n. a." means "not available".

could not change the vertical flux patterns in mangrove-salt marsh ecotone.

Previous study showed that the ratios of the vertical hydraulic conductivity (K_v) to the horizontal hydraulic conductivity (K_h) of the sediments were equal to 2/3, 1, 2, 4 in the silty sand, estuarine mud, clayey sand and surface layer, respectively (Hughes et al., 1998; Xiao et al., 2017). The Mean ± SD (2 ± 1) of the above ratios of K_v:K_h was used to conservatively estimate the horizontal fluxes of nutrients based on the hydraulic gradient between monitoring sites at mangrove/salt marsh and tidal creek. The results showed that all the nutrients had net horizontal effluxes from mangrove and salt marsh to tidal creek. As summed in Table S6, the horizontal fluxes were consistently much less than vertical fluxes with an exception of phosphorus fluxes in mangrove. The total fluxes (the sum of horizontal and vertical fluxes) of nutrients suggested the same source-sink pattern as the individual scenarios that only include vertical fluxes. These results revealed that the horizontal fluxes played a much less role than vertical fluxes, and supported the point in this study that salt marsh can retain high nitrogen loadings discharged from mangrove.

4.4. Ecological and environmental implications

The fluxes across the SWI in the mangrove differed from the salt marsh mainly due to (1) the steeper slope of creek bank and relatively lower water table in the mangrove; and (2) the habitat-specific differences in structures, microbial activities, nutrient cycling and storage. Different wetlands can provide similar ecological functions, but the differences in physiological characteristics and structures likely alter these processes (Kelleway et al., 2017). Salt marshes are herbaceous with seasonal growth patterns (Granville et al., 2021). Finer roots of salt marshes increase the water content and change the redox environment, altering the microbial communities and increasing nitrogen retention (Comeaux et al., 2012; Liu et al., 2020). In contrast, the more labile mangrove litter ultimately leads to much faster mineralization and higher nutrient production (Simpson et al., 2020). Here, the mangrove was a source of NH_4-N being exported to the coastal water. Nutrients promote the productivity of coastal waters and can drive harmful algal blooms (Beman et al., 2005; Mukhopadhyay et al., 2006). The average DIN:DIP mole ratios in surface water were 33 ± 6 in the mangrove and 57 ± 32 in the salt marsh (Fig. S4), well exceeded the Redfield ratio (16:1) but still much lower than average groundwater ratios (497 ± 323) observed in this study. The discharge of groundwater during low tides may promote N-associated eutrophication. The salt marsh sediments served as a sink of nitrogen and had a smaller ratio of DIN:DIP than the mangrove. Hence, the salt marsh can retain nitrogen (especially NH_4-N) that discharged from mangrove, attenuating the nitrogen surplus in the estuarine system. As shown in Fig. 4d, the similar influx of DRP, DOP and TDP in these two habitats suggested that the salt marsh invasion had no significant effect on phosphorus flux patterns in mangroves ($p > 0.05$). Nutrient fluxes (particularly nitrogen) to coastal waters have risen in recent decades in China, resulting in widespread hypoxia and other ecological damages (Howarth et al., 2011). Our findings thus suggest that the invasive expansion of salt marsh may partially alter the nutrient stoichiometry of coastal water and relieve estuarine N-associated eutrophication.

The combined study of hydro-biogeochemical processes in China coastal wetlands advanced our knowledge about how the mangrove-salt marsh ecotone influences estuarine ecosystems. This study provides insights to environmental managers assessing the influences of salt marsh encroachment into mangroves. In other parts of the world such as Australia and the US, mangroves are moving poleward and invading salt marsh areas (Krauss et al., 2011; Osland et al., 2013; Saintilan et al., 2014). This encroachment affects key ecosystem services and function, including increased pressure on salt marsh communities, a greater potential to respond to increasing sea level, changing nitrogen transformations process, and enhanced ability for carbon storage and sequestration (Bianchi et al., 2013; Saintilan et al., 2014; Sullivan et al., 2021). Our investigation builds on this earlier work by showing how changing vegetation communities may influence the wetlands nitrogen cycle. The ongoing mangrove-salt marsh ecotone seemed to reduce ammonium nitrogen exports, alter nutrient ratios and the source-sink pattern of NH_4-N and NO_3-N compared to the native mangrove wetlands. We suggested the ecotone will result in potential shifts of nutrient supply and ratios, modifying phytoplankton growth in coastal waters.

5. Conclusions

Our combination of microbiological, hydrological and biogeochemical approaches revealed that porewater exchange drives the nitrogen source-sink pattern in a mangrove-salt marsh transition zone. The mangrove acted as the net discharge area of groundwater, while the salt marsh acted as the net infiltration area of surface water. Mineralization and DNRA were the main processes for NH_4-N production with higher rates in mangrove sediments. Denitrification dominated NO_3-N removal with the contribution of 97% and 83% in mangrove and salt marsh sediments, respectively. The distributions of functional microbial communities were consistent with the interpretation of nitrogen transformations and fluxes.

The mangrove had a net export of NH_4-N and DON to surface waters, but a net import of NO_x-N and phosphorus due to strong mineralization, denitrification and absorption of phosphorus. The salt marsh had a net import of all forms of nitrogen and phosphorus due to much larger surface water inflow than the groundwater outflow. The mangrove groundwater had a large DIN:DIP mole ratio up to 706 ± 236 due to high NH_4-N concentration. The salt marsh may consume surplus NH_4-N that derived from mangrove groundwater discharge, potentially reducing the nutrient transport to coastal waters through the mangrove-salt marsh ecotone.

The observed contrasting pattern of porewater exchange and nitrogen cycling provides broader insights into the potential ecological implication of the ongoing mangrove-salt marsh ecotone. The ecotone will push these native mangroves from being a source towards a sink of ammonium nitrogen to coastal water by decreasing porewater exchange and modifying the nutrient stoichiometry in this study. Additional observations in other mangrove-salt marsh transition zones are needed to build this view.

CRediT authorship contribution statement

Fenfang Wang: Conceptualization, Data curation, Formal analysis, Investigation, Methodology, Software, Visualization, Writing – original draft. **Kai Xiao:** Investigation, Methodology, Funding acquisition, Project administration, Supervision, Writing – review & editing. **Isaac R. Santos:** Writing – review & editing. **Zeyang Lu:** Investigation, Data curation. **Joseph Tamborski:** Writing – review & editing. **Yao Wang:** Investigation, Software. **Ruifeng Yan:** Investigation. **Nengwang Chen:** Funding acquisition, Methodology, Project administration, Supervision, Writing – review & editing.

Declaration of Competing Interest

The authors declare that they have no known competing financial interests or personal relationships that could have appeared to influence the work reported in this paper.

Acknowledgments

This research was supported by the National Natural Science Foundation of China (Nos. 41976138, 41907162), the Key Laboratory of the Coastal and Wetland Ecosystems (WELRI201601), and the State Key Laboratory of Marine Environmental Science (MELRI1603). IRS is funded by the Swedish Research Council (2020-00457). We thank Junou Du

and Xiuxiu Wang for help in analyzing nutrients and gene abundance, Chenjuan Zheng for organizational help in the lab and Pengbao Wu, Mingzhen Zhang, Zetao Wu for assistance in fieldwork. Our deepest gratitude goes to Dr. M Lafforgue and two anonymous reviewers for their careful work and constructive suggestions that are very helpful to improve our manuscript.

Appendix A. Supplementary data

Supplementary data to this article can be found online at https://doi.org/10.1016/j.jhydrol.2021.127401.

References

An, S.Q., Gu, B.H., Zhou, C.F., Wang, Z.S., Deng, Z.F., Zhi, Y.B., Li, H.L., Chen, L., Yu, D. H., Liu, Y.H., 2007. Spartina invasion in China: implications for invasive species management and future research. Weed Res. 47 (3), 183–191. https://doi.org/10.1111/j.1365-3180.2007.00559.x.

Beman, J.M., Arrigo, K.R., Matson, P.A., 2005. Agricultural runoff fuels large phytoplankton blooms in vulnerable areas of the ocean. Nature 434 (7030), 211–214. https://doi.org/10.1038/nature03370.

Bianchi, T.S., Allison, M.A., Zhao, J., Li, X.X., Comeaux, R.S., Feagin, R.A., Kulawardhana, R.W., 2013. Historical reconstruction of mangrove expansion in the Gulf of Mexico: Linking climate change with carbon sequestration in coastal wetlands. Estuar. Coast. Shelf Sci. 119, 7–16. https://doi.org/10.1016/j.ecss.2012.12.007.

Charette, M.A., 2007. Hydrologic forcing of submarine groundwater discharge: Insight from a seasonal study of radium isotopes in a groundwater-dominated salt marsh estuary. Limnol. Oceanogr. 52 (1), 230–239. https://doi.org/10.4319/lo.2007.52.1.0230.

Chen, N.W., Chen, Z.H., Wu, Y.Q., Hu, A.Y., 2014. Understanding gaseous nitrogen removal through direct measurement of dissolved N_2 and N_2O in a subtropical river-reservoir system. Ecol. Eng. 70, 56–67. https://doi.org/10.1016/j.ecoleng.2014.04.017.

Comeaux, R.S., Allison, M.A., Bianchi, T.S., 2012. Mangrove expansion in the Gulf of Mexico with climate change: Implications for wetland health and resistance to rising sea levels. Estuar. Coast. Shelf Sci. 96, 81–95. https://doi.org/10.1016/j.ecss.2011.10.003.

Cui, L., Sun, H., Du, X., Feng, W., Wang, Y., Zhang, J., Jiang, J., 2021. Dynamics of labile soil organic carbon during the development of mangrove and salt marsh ecosystems. Ecol. Ind. 129, 107875. https://doi.org/10.1016/j.ecolind.2021.107875.

Dale, O.R., Tobias, C.R., Song, B., 2009. Biogeographical distribution of diverse anaerobic ammonium oxidizing (anammox) bacteria in Cape Fear River Estuary. Environ. Microbiol. 11 (5), 1194–1207. https://doi.org/10.1111/j.1462-2920.2008.01850.x.

Dittmar, T., Lara, R.J., 2001. Driving forces behind nutrient and organic matter dynamics in a mangrove tidal creek in North Brazil. Estuar. Coast. Shelf Sci. 52 (2), 249–259. https://doi.org/10.1006/ecss.2000.0743.

Dong, D., Zeng, J., Wei, Z., Yan, J., 2020. Integrating spaceborne optical and SAR imagery for monitoring mangroves and Spartina alterniflora in Zhangjiang Estuary. J. Tropical Oceanography 39 (2), 107–117. https://doi.org/10.11978/2019063.

Feller, I.C., Friess, D.A., Krauss, K.W., Lewis, R.R., 2017. The state of the world's mangroves in the 21st century under climate change. Hydrobiologia 803 (1), 1–12. https://doi.org/10.1007/s10750-017-3331-z.

Feng, J.X., Zhou, J., Wang, L.M., Cui, X.W., Ning, C.X., Wu, H., Zhu, X.S., Lin, G.H., 2017. Effects of short-term invasion of Spartina alterniflora and the subsequent restoration of native mangroves on the soil organic carbon, nitrogen and phosphorus stock. Chemosphere 184, 774–783. https://doi.org/10.1016/j.chemosphere.2017.06.060.

Gao, D.Z., Li, X.F., Lin, X.B., Wu, D.M., Jin, B.S., Huang, Y.P., Liu, M., Chen, X., 2017. Soil dissimilatory nitrate reduction processes in the Spartina alterniflora invasion chronosequences of a coastal wetland of southeastern China: Dynamics and environmental implications. Plant Soil 421 (1–2), 383–399. https://doi.org/10.1007/s11104-017-3464-x.

Gao, G.F., Li, P.F., Zhong, J.X., Shen, Z.J., Chen, J., Li, Y.T., Isabwe, A., Zhu, X.Y., Ding, Q.S., Zhang, S., Gao, C.H., Zheng, H.L., 2019. Spartina alterniflora invasion alters soil bacterial communities and enhances soil N_2O emissions by stimulating soil denitrification in mangrove wetland. Sci. Total Environ. 653, 231–240. https://doi.org/10.1016/j.scitotenv.2018.10.277.

Gleeson, J., Santos, I.R., Maher, D.T., Golsby-Smith, L., 2013. Groundwater-surface water exchange in a mangrove tidal creek: Evidence from natural geochemical tracers and implications for nutrient budgets. Mar. Chem. 156, 27–37. https://doi.org/10.1016/j.marchem.2013.02.001.

Gonneea, M.E., Charette, M.A., 2014. Hydrologic controls on nutrient cycling in an unconfined coastal aquifer. Environ. Sci. Technol. 48 (24), 14178–14185. https://doi.org/10.1021/es503313t.

Granville, K.E., Ooi, S.K., Koenig, L.E., Lawrence, B.A., Elphick, C.S., Helton, A.M., 2021. Seasonal patterns of denitrification and N_2O production in a Southern New England salt marsh. Wetlands. 41 (1) https://doi.org/10.1007/s13157-021-01393-x.

Holmboe, N., Kristensen, E., Andersen, F.O., 2001. Anoxic decomposition in sediments from a tropical mangrove forest and the temperate Wadden Sea: Implications of N and P addition experiments. Estuar. Coast. Shelf Sci. 53 (2), 125–140. https://doi.org/10.1006/ecss.2000.0794.

Hou, L., Li, H., Zheng, C., Ma, Q., Wang, C., Wang, X., Qu, W., 2016. Seawater-groundwater exchange in a silty tidal flat in the South Coast of Laizhou Bay, China. J. Coastal Res. 74, 136–148.

Howarth, R., Chan, F., Conley, D.J., Garnier, J., Doney, S.C., Marino, R., Billen, G., 2011. Coupled biogeochemical cycles: eutrophication and hypoxia in temperate estuaries and coastal marine ecosystems. Front. Ecol. Environ. 9 (1), 18–26. https://doi.org/10.1890/100008.

Hughes, C.E., Binning, P., Willgoose, G.R., 1998. Characterisation of the hydrology of an estuarine wetland. J. Hydrol. 211 (1–4), 34–49. https://doi.org/10.1016/s0022-1694(98)00194-2.

Kelleway, J.J., Cavanaugh, K., Rogers, K., Feller, I.C., Ens, E., Doughty, C., Saintilan, N., 2017. Review of the ecosystem service implications of mangrove encroachment into salt marshes. Glob. Change Biol. 23 (10), 3967–3983. https://doi.org/10.1111/gcb.13727.

Krauss, K.W., From, A.S., Doyle, T.W., Doyle, T.J., Barry, M.J., 2011. Sea-level rise and landscape change influence mangrove encroachment onto marsh in the Ten Thousand Islands region of Florida, USA. J. Coastal Conserv. 15 (4), 629–638. https://doi.org/10.1007/s11852-011-0153-4.

Krest, J.M., Moore, W.S., Gardner, L.R., Morris, J.T., 2000. Marsh nutrient export supplied by groundwater discharge: Evidence from radium measurements. Global Biogeochem. Cycles 14 (1), 167–176. https://doi.org/10.1029/1999gb001197.

Lee, R.Y., Porubsky, W.P., Feller, I.C., McKee, K.L., Joye, S.B., 2008. Porewater biogeochemistry and soil metabolism in dwarf red mangrove habitats (Twin Cays, Belize). Biogeochemistry 87 (2), 181–198. https://doi.org/10.1007/s10533-008-9176-9.

Li, G., Li, H.L., Wang, X.J., Qu, W.J., Zhang, Y., Xiao, K., Luo, M.H., Zheng, C.M., 2018. Groundwater-surface water exchanges and associated nutrient fluxes in Dan'ao Estuary, Daya Bay, China. Continental Shelf Res. 166, 83–91. https://doi.org/10.1016/j.csr.2018.06.014.

Lin, X., Hou, L., Liu, M., Li, X., Zheng, Y., Yin, G., Gao, J., Jiang, X., 2016. Nitrogen mineralization and immobilization in sediments of the East China Sea: Spatiotemporal variations and environmental implications. J. Geophys. Res.-Biogeosci. 121 (11), 2842–2855.

Lin, X., Lu, K., Hardison, A.K., Liu, Z., Xu, X., Gao, D., Gong, J., Gardner, W.S., 2021. New membrane inlet mass spectrometry method (REOX/MIMS) to measure ^{15}N-nitrate in isotope-enrichment experiments: analytical technique and applications. Ecological Indicartors. 126, 107639. https://doi.org/10.1016/j.ecolind.2021.107639.

Lisa, J.A., Song, B., Tobias, C.R., Duernberger, K.A., 2014. Impacts of freshwater flushing on anammox community structure and activities in the New River Estuary, USA. Aquat. Microb. Ecol. 72 (1), 17–31. https://doi.org/10.3354/ame01682.

Liu, H., Xu, X., Zhou, C.H., Zhao, J.Y., Li, B., Nie, M., 2020. Geographic linkages of root traits to salt marsh productivity. Ecosystems 24 (3), 726–737. https://doi.org/10.1007/s10021-020-00546-z.

Luvizott, D.M., Araujo, J.E., Silva, M.D.P., Dias, A.C.F., Kraft, B., Tegetmeye, H., Strous, M., Andreote, F.D., 2019. The rates and players of denitrification, dissimilatory nitrate reduction to ammonia (DNRA) and anaerobic ammonia oxidation (anammox) in mangrove soils. Anais Da Academia Brasileira De Ciencias 91, 14. https://doi.org/10.1590/0001-3765201820180373.

McKee, K.L., Vervaeke, W.C., 2018. Will fluctuations in salt marsh-mangrove dominance alter vulnerability of a subtropical wetland to sea-level rise? Glob. Change Biol. 24 (3), 1224–1238. https://doi.org/10.1111/gcb.13945.

Meng, Y., He, Z., Liu, B., Chen, L., Lin, P., Luo, W., 2020. Soil salinity and moisture control the processes of soil nitrification and denitrification in a riparian wetlands in an extremely arid regions in Northwestern China. Water 12 (10), 2815. https://doi.org/10.3390/w12102815.

Moore, W.S., 2010. A reevaluation of submarine groundwater discharge along the southeastern coast of North America. Global Biogeochem. Cycles 24 (4), n/a–n/a.

Mukhopadhyay, S.K., Biswas, H., De, T.K., Jana, T.K., 2006. Fluxes of nutrients from the tropical River Hooghly at the land-ocean boundary of Sundarbans, NE Coast of Bay of Bengal, India. J. Marine Systems 62 (1–2), 9–21. https://doi.org/10.1016/j.jmarsys.2006.03.004.

Osland, M.J., Enwright, N., Day, R.H., Doyle, T.W., 2013. Winter climate change and coastal wetland foundation species: salt marshes versus mangrove forests in the southeastern United States. Glob. Change Biol. 19, 1482–1494. https://doi.org/10.1111/gcb.12126.

Pezeshki, S.R., 2001. Wetland plant responses to soil flooding. Environ. Exp. Bot. 46 (3), 299–312. https://doi.org/10.1016/s0098-8472(01)00107-1.

Qu, W.J., Li, H.L., Huang, H., Zheng, C.M., Wang, C.Y., Wang, X.J., Zhang, Y., 2017. Seawater-groundwater exchange and nutrients carried by submarine groundwater discharge in different types of wetlands at Jiaozhou Bay, China. J. Hydrol. 555, 185–197. https://doi.org/10.1016/j.jhydrol.2017.10.014.

Ranjan, R.K., Ramanathan, A.L., Chauhan, R., Singh, G., 2011. Phosphorus fractionation in sediments of the Pichavaram mangrove ecosystem, south-eastern coast of India. Environ. Earth Sci. 62 (8), 1779–1787. https://doi.org/10.1007/s12665-010-0659-3.

Reithmaier, G.M.S., Chen, X., Santos, I.R., Drexl, M.J., Holloway, C., Call, M., Álvarez, P. G., Euler, S., Maher, D.T., 2021. Rainfall drives rapid shifts in carbon and nutrient source-sink dynamics of an urbanised, mangrove-fringed estuary. Estuar. Coast. Shelf Sci. 249, 107064. https://doi.org/10.1016/j.ecss.2020.107064.

Risgaard-Petersen, N., Nielsen, L.P., Rysgaard, S., Dalsgaard, T., Meyer, R.L., 2003. Application of the isotope pairing technique in sediments where anammox and denitrification coexist. Limnol. Oceanography-Methods 1, 63–73. https://doi.org/10.4319/lom.2011.1.63.

Robinson, C., Li, L., Prommer, H., 2007. Tide-induced recirculation across the aquifer-ocean interface. Water Resour. Res. 43 (7), 14. https://doi.org/10.1029/2006wr005679.

Rogers, K., Kelleway, J.J., Saintilan, N., Megonigal, J.P., Adams, J.B., Holmquist, J.R., Lu, M., Schile-Beers, L., Zawadzki, A., Mazumder, D., Woodroffe, C.D., 2019. Wetland carbon storage controlled by millennial-scale variation in relative sea-level rise. Nature 567 (7746), 91–95. https://doi.org/10.1038/s41586-019-0951-7.

Sadat-Noori, M., Glamore, W., 2019. Porewater exchange drives trace metal, dissolved organic carbon and total dissolved nitrogen export from a temperate mangrove wetland. J. Environ. Manage. 248, 11. https://doi.org/10.1016/j.jenvman.2019.109264.

Saintilan, N., Wilson, N.C., Rogers, K., Rajkaran, A., Krauss, K.W., 2014. Mangrove expansion and salt marsh decline at mangrove poleward limits. Glob. Change Biol. 20 (1), 147–157. https://doi.org/10.1111/gcb.12341.

Santos, I.R., Bryan, K.R., Pilditch, C.A., Tait, D.R., 2014. Influence of porewater exchange on nutrient dynamics in two New Zealand estuarine intertidal flats. Mar. Chem. 167, 57–70. https://doi.org/10.1016/j.marchem.2014.04.006.

Santos, I.R., Maher, D.T., Larkin, R., Webb, J.R., Sanders, C.J., 2019. Carbon outwelling and outgassing vs. burial in an estuarine tidal creek surrounded by mangrove and saltmarsh wetlands. Limnol. Oceanogr. 64 (3), 996–1013. https://doi.org/10.1002/lno.11090.

Schutte, C. A., Ahmerkamp, S., Wu, C. S., Seidel, M., de Beer, D., Cook, P. L. M., & Joye, S. B. (2019). Biogeochemical Dynamics of Coastal Tidal Flats, 407-440 pp., doi :10.1016/b978-0-444-63893-9.00012-5.

Sharp, S.J., Elgersma, K.J., Martina, J.P., Currie, W.S., 2021. Hydrologic flushing rates drive nitrogen cycling and plant invasion in a freshwater coastal wetland model. Ecol. Appl. 31 (2), 17. https://doi.org/10.1002/eap.2233.

Shen, L.-D., Wu, H.-S., Liu, X., Li, J., 2017. Vertical distribution and activity of anaerobic ammonium-oxidising bacteria in a vegetable field. Geoderma 288, 56–63. https://doi.org/10.1016/j.geoderma.2016.11.007.

Simpson, L.T., Cherry, J.A., Smith, R.S., Feller, I.C., 2020. Mangrove encroachment alters decomposition rate in saltmarsh through changes in litter quality. Ecosystems 24 (4), 840–854. https://doi.org/10.1007/s10021-020-00554-z.

Slomp, C.P., Van Cappellen, P., 2004. Nutrient inputs to the coastal ocean through submarine groundwater discharge: controls and potential impact. J. Hydrol. 295 (1–4), 64–86. https://doi.org/10.1016/j.jhydrol.2004.02.018.

Smith, C.J., Dong, L.F., Wilson, J., Stott, A., Osborn, A.M., Nedwell, D.B., 2015. Seasonal variation in denitrification and dissimilatory nitrate reduction to ammonia process rates and corresponding key functional genes along an estuarine nitrate gradient. Front. Microbiol. 6 (542) https://doi.org/10.3389/fmicb.2015.00542.

Smolders, E., Baetens, E., Verbeeck, M., Nawara, S., Diels, J., Verdievel, M., Peeters, B., De Cooman, W., Baken, S., 2017. Internal loading and redox cycling of sediment iron explain reactive phosphorus concentrations in lowland rivers. Environ. Sci. Technol. 51 (5), 2584–2592. https://doi.org/10.1021/acs.est.6b0433710.1021/acs.est.6b04337.s001.

Steinlein, T., 2013. Invasive alien plants and their effects on native microbial soil communities. In: Progress in Botany: Vol. 74. edited by U. Lüttge, W. Beyschlag, D. Francis and J. Cushman, pp. 293-319, Springer Berlin Heidelberg, Berlin, Heidelberg, doi:10.1007/978-3-642-30967-0_11.

Steinmuller, H.E., Foster, T.E., Boudreau, P., Hinkle, C.R., Chambers, L.G., 2020. Tipping points in the mangrove march: characterization of biogeochemical cycling along the mangrove-salt marsh ecotone. Ecosystems 23 (2), 417–434. https://doi.org/10.1007/s10021-019-00411-8.

Sullivan, C.R., Smyth, A.R., Martin, C.W., Reynolds, L.K., 2021. How does mangrove expansion affect structure and function of adjacent seagrass meadows? Estuaries Coasts 44 (2), 453–467. https://doi.org/10.1007/s12237-020-00879-x.

Tait, D.R., Maher, D.T., Sanders, C.J., Santos, I.R., 2017. Radium-derived porewater exchange and dissolved N and P fluxes in mangroves. Geochim. Cosmochim. Acta 200, 295–309. https://doi.org/10.1016/j.gca.2016.12.024.

Tamborski, J.J., Eagle, M., Kurylyk, B.L., Kroeger, K.D., Wang, Z.A., Henderson, P., Charette, M.A., 2021. Pore water exchange-driven inorganic carbon export from intertidal salt marshes. Limnol. Oceanogr. 66 (5), 1774–1792. https://doi.org/10.1002/lno.11721.

Taniguchi, M., 2002. Tidal effects on submarine groundwater discharge into the ocean. Geophys. Res. Lett. 29 (12), 3. https://doi.org/10.1029/2002gl014987.

Taniguchi, M., Dulai, H., Burnett, K.M., Santos, I.R., Sugimoto, R., Stieglitz, T., Kim, G., Moosdorf, N., Burnett, W.C., 2019. Submarine groundwater discharge: updates on its measurement techniques, geophysical drivers, magnitudes, and effects. Front. Environ. Sci. 7, 26. https://doi.org/10.3389/fenvs.2019.00141.

Wadnerkar, P.D., Batsaikhan, B., Conrad, S.R., Davis, K., Correa, R.E., Holloway, C., White, S.A., Sanders, C.J., Santos, I.R., 2021. Contrasting radium-derived groundwater exchange and nutrient lateral fluxes in a natural mangrove versus an Artificial Canal. Estuaries Coasts 44 (1), 123–136. https://doi.org/10.1007/s12237-020-00778-1.

Wadnerkar, P.D., Santos, I.R., Looman, A., Sanders, C.J., White, S., Tucker, J.P., Holloway, C., 2019. Significant nitrate attenuation in a mangrove-fringed estuary during a flood-chase experiment. Environ. Pollut. 253, 1000–1008. https://doi.org/10.1016/j.envpol.2019.06.060.

Wang, F.F., Cheng, P., Chen, N.W., Kuo, Y.-M., 2021. Tidal driven nutrient exchange between mangroves and estuary reveals a dynamic source-sink pattern. Chemosphere 270, 128665. https://doi.org/10.1016/j.chemosphere.2020.128665.

Wang, F.F., Chen, N.W., Yan, J., Lin, J.J., Guo, W.D., Cheng, P., Liu, Q., Huang, B.Q., Tian, Y., 2019. Major processes shaping mangroves as inorganic nitrogen sources or sinks: insights from a multidisciplinary study. J. Geophys. Res.-Biogeosci. 124 (5), 1194–1208. https://doi.org/10.1029/2018jg004875.

Wang, H.T., Su, J.Q., Zheng, T.L., Yang, X.R., 2014. Impacts of vegetation, tidal process, and depth on the activities, abundances, and community compositions of denitrifiers in mangrove sediment. Appl. Microbiol. Biotechnol. 98 (22), 9375–9387. https://doi.org/10.1007/s00253-014-6017-8.

Xiao, K., Li, G., Li, H.L., Zhang, Y., Wang, X.J., Hu, W.L., Zhang, C.C., 2019. Combining hydrological investigations and radium isotopes to understand the environmental effect of groundwater discharge to a typical urbanized estuary in China. Sci. Total Environ. 695, 15. https://doi.org/10.1016/j.scitotenv.2019.133872.

Xiao, K., Li, H.L., Wilson, A.M., Xia, Y.Q., Wan, L., Zheng, C.M., Ma, Q., Wang, C.Y., Wang, X.S., Jiang, X.W., 2017. Tidal groundwater flow and its ecological effects in a brackish marsh at the mouth of a large sub-tropical river. J. Hydrol. 555, 198–212. https://doi.org/10.1016/j.jhydrol.2017.10.025.

Xiao, K., Wu, J.P., Li, H.L., Hong, Y.G., Wilson, A.M., Jiao, J.J., Shananan, M., 2018. Nitrogen fate in a subtropical mangrove swamp: Potential association with seawater-groundwater exchange. Sci. Total Environ. 635, 586–597. https://doi.org/10.1016/j.scitotenv.2018.04.143.

Yang, W., Zhao, H., Chen, X.L., Yin, S.L., Cheng, X.L., An, S.Q., 2013. Consequences of short-term C-4 plant Spartina alterniflora invasions for soil organic carbon dynamics in a coastal wetland of Eastern China. Ecol. Eng. 61, 50–57. https://doi.org/10.1016/j.ecoleng.2013.09.056.

Yin, G., Hou, L., Zong, H., Ding, P., Liu, M., Zhang, S., Cheng, X., Zhou, J., 2015. Denitrification and anaerobic ammonium oxidization across the sediment-water Interface in the hypereutrophic ecosystem, Jinpu Bay, in the Northeastern Coast of China. Estuaries Coasts 38 (1), 211–219. https://doi.org/10.1007/s12237-014-9798-1.

Zhang, M., Dai, P., Lin, X., Lin, Li'an, Hetharua, B., Zhang, Y., Tian, Y., 2020. Nitrogen loss by anaerobic ammonium oxidation in a mangrove wetland of the Zhangjiang Estuary, China. Sci. Total Environ. 698, 134291. https://doi.org/10.1016/j.scitotenv.2019.134291.

Zhang, Q.F., Peng, J.J., Chen, Q., Li, X.F., Xu, C.Y., Yin, H.B., Yu, S., 2011. Impacts of Spartina alterniflora invasion on abundance and composition of ammonia oxidizers in estuarine sediment. J. Soils Sediments 11 (6), 1020–1031. https://doi.org/10.1007/s11368-011-0369-9.

Zhang, Y.H., Huang, G.M., Wang, W.Q., Chen, L.Z., Lin, G.H., 2012. Interactions between mangroves and exotic Spartina in an anthropogenically disturbed estuary in southern China. Ecology 93 (3), 588–597. https://doi.org/10.1890/11-1302.1.

Zhu, X.D., Hou, Y.W., Weng, Q.H., Chen, L.Z., 2019. Integrating UAV optical imagery and LiDAR data for assessing the spatial relationship between mangrove and inundation across a subtropical estuarine wetland. ISPRS J. Photogramm. Remote Sens. 149, 146–156. https://doi.org/10.1016/j.isprsjprs.2019.01.021.